

Pressure and Squeeze Effects on the Dynamic Characteristics of Elastomer O-Rings Under Small Reciprocating Motion

I. Green¹

I. Etsion
Mem. ASME

Department of Mechanical Engineering,
Technion, Haifa 32000, Israel

A test procedure is described by which quick measurements of stiffness and damping coefficients of elastomer O-rings can be made for a wide range of the parameters affecting O-ring dynamics. Tests were performed to investigate the effects of squeeze and pressure on the dynamic characteristics of Nitrile (Buna N) and Fluorocarbon (Viton 75) O-rings. Results of these tests are presented and discussed.

Introduction

An O-ring seal is a means for closing off a passageway preventing an unwanted escape or loss of fluid. The scope of O-ring seal use is quite wide including both static and dynamic applications. By far the greatest dynamic use of O-rings is in reciprocating seals where relative reciprocating motion (along the shaft axis) takes place between the inner and outer elements. This motion tends to slide or roll the O-ring back and forth with the reciprocation. Examples of a reciprocating seal would be a piston in a cylinder, a plunger entering a chamber, a hydraulic or pneumatic actuator, etc. Usually, the axial motion is of relatively large amplitude where the piston, plunger or actuator move from one equilibrium position to another and then stay still. However, in many cases, especially in fast response control systems, high frequency small amplitude fluctuations take place about the equilibrium position and result in very small amplitude reciprocating motion of the O-rings. In other cases, e.g. mechanical face seals, the small reciprocating motion is the only motion of the O-rings. The small amplitude reciprocating motion described above plays an important role in the dynamics of the systems concerned, and can strongly affect their performance. Obviously the dynamic properties of the O-rings is an important factor in such systems behavior. Unfortunately very little information is available in the literature on O-ring dynamics.

A very good source on dynamic properties of elastomers in general is given in reference [1]. A main conclusion emerging from this source is that no solid theoretical prediction on elastomers dynamic characteristics is available at present. Stiffness and damping coefficients can be found experimentally and are affected by many factors such as composition, geometry, frequency, temperature, strain and preload.

While a great deal of information has been gathered on

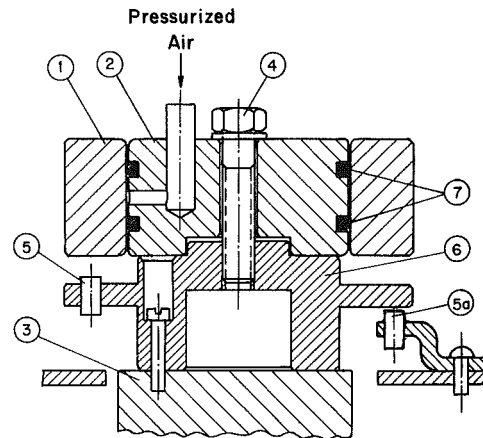


Fig. 1 Test rig components

various elastomer springs and dampers this is not the case for O-rings. References [2] and [3] present results on measured dynamic properties of elastomer O-rings under reciprocating unidirectional radial squeeze, similar to the mode of application in squeeze film dampers. In references [4] and [5] axial forces transmitted by O-rings subjected to a reciprocating drag were measured for various amplitudes and frequencies. However, for a general dynamic analysis of a reciprocating system, the stiffness and damping coefficients of the O-ring, not the forces, are required. Reference [6] describes a test procedure and presents some results of measured dynamic properties of elastomer O-rings subjected to small reciprocating axial motion. The test was performed at ambient pressure and with the nominal squeeze recommended for industrial O-ring static seals [7]. Stiffness and damping coefficients were measured in [6] at ten different discrete frequencies in the range 100 Hz to 300 Hz. This is a lengthy procedure which consumes a lot of time if the effect of other parameters, in addition to the frequency, is desired.

The purpose of the present work is twofold: (a) to investigate the effect of various squeeze levels and different pressures on the dynamic properties of the reciprocating O-

¹Currently with Georgia Institute of Technology, Atlanta, GA 30332
Contributed by the Tribology Division of THE AMERICAN SOCIETY OF MECHANICAL ENGINEERS and presented at the ASME/ASLE Joint Tribology Conference, Atlanta Ga., October 8-10, 1985. Manuscript received by the Tribology Division February 28, 1985. Paper No. 85-Trib-5.

Table 1 Actual effective squeeze values

O-ring Cross section Diameter W mm (in)	Squeeze level $S\%$		
	Low S_l	Medium S_m	High S_h
1.78 (1/16)	11	20	27
3.53 (1/8)	13	19.5	29
5.33 (3/16)	10	19	29

rings, and (b) to introduce a relatively simple test procedure that will allow quick and reliable measurements of the dynamic properties for a wide range of the important parameters.

Experimental Setup and Test Procedure

The Base Excitation Resonant Mass (BERM) test method (see reference [1] and [6]) was selected for the present investigation. A Kelvin-Voigt model is assumed for the elastomer O-ring which is held in a vibrating base and supports a given mass. The stiffness and damping coefficients of the O-ring at any vibration frequency can be found from independent measurements of the mass response to the base motion.

A test rig was set up as shown in Fig. 1 to obtain the stiffness and damping coefficients of elastomer O-rings subjected to small reciprocating axial motion. A holder (6) attached to a vibrating table (3) of an electromagnetic shaker is holding a base (2) by means of a single screw (4), thus, allowing quick assemble and disassemble. Nine different base sizes were used to allow three squeeze levels for three different O-ring sizes. Each base accommodates a pair of O-rings (7) having mean outer diameter of 76.2 mm (3 in.). Three different nominal cross section diameters were tested: 1.78 mm, 3.53 mm, and 5.33 mm (1/16 in., 1/8 in., and 3/16 in.). A mass of 2.014 kg in the form of an annular ring (1) is fitted on the O-rings. The diametral clearance between the O-ring gland O.D. and the ring (1) was 0.050 mm for the 1/16 in. O-ring and 0.075 mm for the 1/8 in. and 3/16 in. O-rings. The selected sizes of the O-rings grooves in the various bases and the inner diameter of the annular ring gave three levels of squeeze for every nominal cross section size of the O-rings. A low squeeze level of 10 percent, medium squeeze level of 20 percent, and high squeeze level of 30 percent were selected for the tests. However, because of manufacturing tolerances the actual effective squeeze values differ somewhat from the nominal ones. Table 1 presents the various effective squeeze levels that were actually tested. It should be noted that the calculated effective squeeze takes into consideration the stretch of the O-ring in its groove (see Appendix A).

Pressurized air is supplied through the base (2) into the cavity between the two O-rings, hence, allowing tests to be carried out under various pressures. In preliminary tests it was found that the system becomes very stiff when pressurized to 0.5 MPa (75 psi) or above. With the existing setup it was difficult to obtain good results, thus, maximum pressure was limited to 0.4 MPa.

Two eddy current proximity probes (5) and (5a) are used to

measure the base motion $y = y(t)$ and the mass response $x = x(t)$ relative to the base, respectively. A data acquisition system based on a PDP 11/40 minicomputer was used to record the probes output and to analyze the data. The two signals $y(t)$ and $x(t)$ were sampled at a rate of 1000 Hz after proper filtration and amplification. A noise generator was used to excite the shaker. By selecting a white noise for the input to the shaker a wide spectrum of frequencies ω_i was included in both $y(t)$ and $x(t)$ which can be described in the form

$$y = \sum_{i=1}^n y_{0i} \sin(\omega_i t + \phi_i) \quad (1)$$

$$x = \sum_{i=1}^n x_{0i} \sin \omega_i t \quad (2)$$

A low pass filter and a high pass filter were used to contain the range of frequencies between 80 Hz and 400 Hz. This was done merely for practical reasons to avoid natural frequencies of the test rig. A spectral analysis code (see Appendix B) was used to identify at each frequency ω the corresponding amplitudes ratio, x_0/y_0 , and the phase shift ϕ . The stiffness and damping coefficients were then calculated from the relations (see reference [6])

$$D = m\omega \frac{\sin \phi}{\alpha} \quad (3)$$

$$K = m\omega^2 \left(\frac{\cos \phi}{\alpha} + 1 \right) \quad (4)$$

where m is the mass of the annular ring and α is the transmissibility x_0/y_0 corresponding to a given frequency ω . Finally, a least square procedure was utilized to find a best fit for the collection of data points. This provided expressions for the stiffness and damping in the exponential form

$$K = A\omega^B \quad (5)$$

and

$$D = a\omega^b \quad (6)$$

where A , B , a , and b are constants related to the elastomer material, to the O-ring geometry, and to the squeeze level and system pressure. The amplitudes y_0 and x_0 were of the order of 10 μm and therefore their effect on the stiffness and damping is negligible [6].

Results and Discussion

Two different O-ring materials, Nitrile (Buna N) and Fluorocarbon (Viton 75), were tested. Their durometer hardness was 70 and 75, respectively. A spectral analysis (see Appendix B) was used to reduce the data. Of the many test results accumulated only those (about 90 percent) that gave a coherence function value (see Appendix B) greater than 0.8 were considered successful. These results were summarized in Tables 2 and 3 for three representative gage pressures namely, 0, 0.2 and 0.4 MPa. At the highest squeeze level tests were performed at ambient pressure only because the system became too stiff. The results presented in the tables are in the form of the constants A , B , a , and b corresponding to equations (5) and (6). Also given in the tables are the values of

Nomenclature

A, a = constants	m = mass	x_0 = mass amplitude relative to base
B, b = constants	P = pressure	y = base displacement
D = damping coefficients	t = time	y_0 = base amplitude
f = frequency, Hz	W = O-ring diameter	α = transmissibility, x_0/y_0
K = stiffness coefficient	x = mass displacement relative to base	ϕ = phase shift
		ω = frequency, rad/s

Table 2 Summary of the results for Nitril (Buna N) O-ring

<i>S</i>	<i>W</i> mm	<i>P</i> MPa	$A \times 10^{-5}$	<i>B</i>	K_{200} MN/m	<i>a</i>	<i>b</i>	D_{200} Ns/m
0.11	1.78	0.0	0.266	0.486	0.85	31.5	0.358	405
		0.2	4.333	0.214	2.00	177.7	0.184	661
		0.4	4.423	0.237	2.40	180.7	0.194	721
0.13	3.53	0.0	1.085	0.121	0.26	20.4	0.398	349
		0.2	3.902	0.238	2.13	275.4	0.123	663
		0.4	6.550	0.204	2.81	243.1	0.157	745
0.10	5.33	0.0	0.281	0.290	0.22	28.5	0.348	341
		0.2	0.832	0.230	0.43	5.1	0.633	576
		0.4	4.689	0.241	2.62	350.7	0.118	814
0.20	1.78	0.0	0.743	0.418	1.47	244.3	0.128	609
		0.2	1.596	0.322	1.59	145.1	0.227	733
		0.4	5.993	0.226	3.00	33.3	0.463	907
0.20	3.53	0.0	0.827	0.281	0.61	20.4	0.433	449
		0.2	4.397	0.170	1.48	105.7	0.274	747
		0.4	3.753	0.299	3.17	779.4	0.035	1001
0.19	5.33	0.0	2.619	0.123	0.63	29.7	0.388	474
		0.2	2.515	0.250	1.50	167.5	0.226	840
		0.4	1.843	0.425	3.83	590.6	0.109	1286
0.29	3.53	0.0	10.37	0.134	2.70	291.5	0.158	900
0.29	5.33	0.0	4.62	0.195	1.86	935.1	0.003	853

Table 3 Summary of the results for Fluorocarbon (Viton 75) O-ring

<i>S</i>	<i>W</i> mm	<i>P</i> MPa	$A \times 10^{-4}$	<i>B</i>	K_{200} MN/m	$a \times 10^{-4}$	<i>b</i>	D_{200} Ns/m
0.11	1.78	0.0	4.295	0.530	1.89	0.477	-0.131	1872
		0.2	4.839	0.613	3.84	1.786	-0.253	2963
		0.4	12.45	0.597	8.82	13.40	-0.450	5401
0.13	3.53	0.0	30.71	0.197	1.25	0.226	-0.059	1486
		0.2	4.506	0.642	4.40	1.675	-0.227	3315
		0.4	6.591	0.621	5.84	4.017	-0.317	4183
0.10	5.33	0.0	42.85	0.131	1.10	0.110	0.0	1100
		0.2	1.149	0.699	1.69	1.144	-0.240	2064
		0.4	5.522	0.607	4.20	1.978	-0.263	3028
0.20	1.78	0.0	5.632	0.617	4.60	1.249	-0.161	3959
		0.2	5.533	0.639	5.29	1.773	-0.194	4441
		0.4	7.382	0.680	9.45	3.063	-0.202	7246
0.20	3.53	0.0	5.444	0.471	1.57	0.135	-0.010	1261
		0.2	8.930	0.565	5.03	1.287	-0.173	3745
		0.4	16.51	0.578	10.20	4.354	-0.271	6295
0.19	5.33	0.0	7.313	0.466	2.03	0.273	-0.044	2000
		0.2	5.444	0.522	2.26	0.361	-0.070	2192
		0.4	8.677	0.640	8.35	2.569	-0.183	6960
0.27	1.78	0.0	11.74	0.544	5.70	0.295	-0.277	4088
0.29	3.53	0.0	5.924	0.603	4.38	0.130	-0.190	3358
0.29	5.33	0.0	5.550	0.586	3.63	0.641	-0.111	2903

the stiffness coefficient K_{200} and damping coefficient D_{200} corresponding to a frequency, f , of 200 Hz.

Figures 2-5 show the squeeze effect on K and D at the zero pressure level, and the pressure effect on K and D at the medium squeeze level. The effects at different squeeze and pressure levels are similar to those shown in Figs. 2-5.

Figure 2a shows the effect of squeeze on the stiffness coefficient of Buna N O-rings at zero pressure. It can be seen that the results for the medium and large cross section diameters are very close at each one of the three squeeze levels.

This may indicate that the cross section diameter is not a significant factor in the stiffness coefficient K . The small cross section diameter, however, shows more erratic behavior with larger stiffness. The slope of the straight lines in Fig. 2(a) is quite similar. Thus, it can be concluded that the constant B (equation (5)) is not very much effected by either the squeeze level or the cross section diameter. Indeed from Table 2 it can be seen that most of the results for B fall in the range of 0.195 to 0.299.

Figure 2(b) shows the effect of squeeze on the damping

coefficient of the Buna N O-rings at zero pressure. Here again the two larger cross section diameters gave very similar results. The slope of the lines, namely the constant b , is also very similar for the various squeeze levels as was found in the case of the stiffness coefficient.

Figures 3(a) and 3(b) show the effect of pressure on the stiffness and damping coefficients of Buna N O-rings at the medium squeeze level. The results here are less conclusive but with a few exceptions it can be seen that the pressure does not affect significantly the constants B and b . Increasing the pressure increases both the stiffness and the damping.

Figures 4(a) and 4(b) show the effect of squeeze at $p = 0$ on the stiffness and damping coefficients of Viton 75 O-rings. The behavior is similar to that of the Buna N O-rings and is even more regular as far as the slopes of the lines, namely the constants B , and b , are concerned. Again one can see that these constants are almost unaffected by the squeeze level. Similar trends are shown in Figs. 5(a) and 5(b) presenting the effect of pressure on the stiffness and damping coefficients of Viton 75 O-rings at the medium squeeze level.

In general it can be seen that increasing the pressure or the

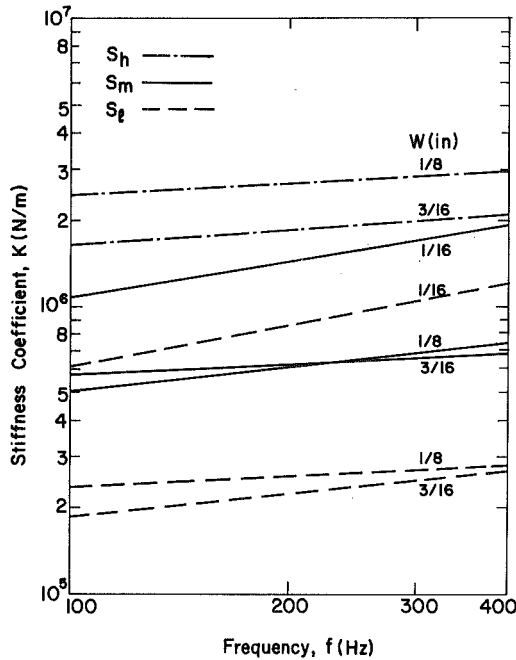


Fig. 2(a) Effect of squeeze, S , on the stiffness coefficient, K , of Buna-N O-rings, $P = 0.0$

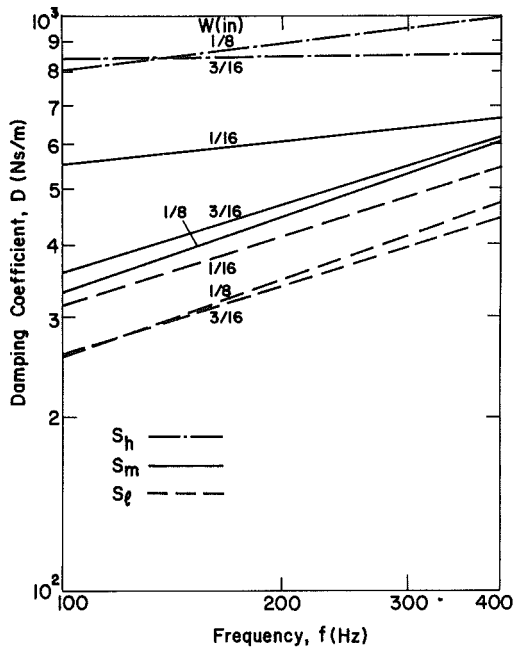


Fig. 2(b) Effect of squeeze, S , on the damping coefficient, D , of Buna-N O-rings, $P = 0.0$

squeeze increases both the stiffness and the damping coefficients at a given frequency. The squeeze or pressure levels have little effect on the exponents B and b of equations (5) and (6). With the exception of the smallest cross section diameter (1/16 in.) it seems that the cross section diameter does not affect significantly the stiffness and damping coefficients. This point, however, has to be examined more carefully. With the present test rig, and especially at the high squeeze level, a substantial amount of force is required to slide the mass over the O-rings during assembly. The O-rings could have been initially twisted when the mass was fitted over them. The smallest cross section diameter seems to be more prone to such a twist which may partly explain the less regular results obtained with this O-ring size.

Another source of uncertainty may result from the need to

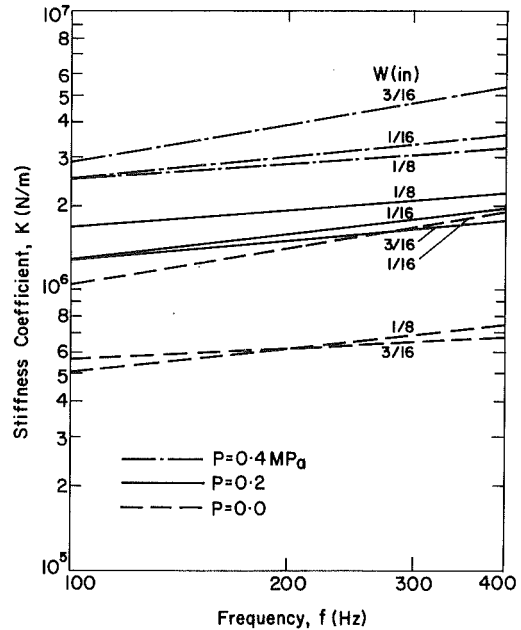


Fig. 3(a) Effect of pressure, P , on the stiffness coefficient, K , of Buna-N O-rings, $S = S_m$

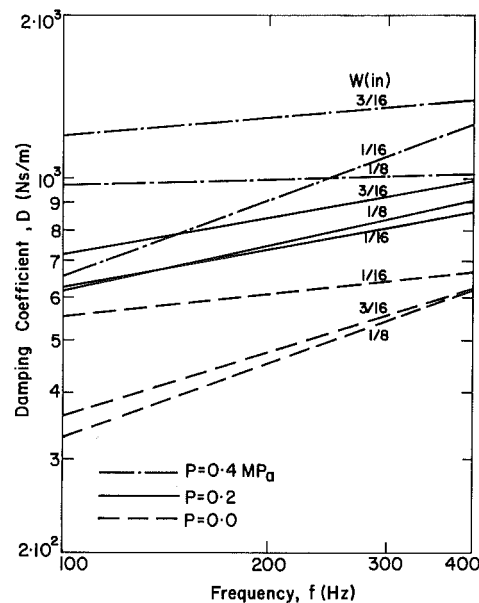


Fig. 3(b) Effect of pressure, P , on the damping coefficient, D , of Buna-N O-rings, $S = S_m$

lubricate the O-rings and inner surface of the mass in order to allow assembly without damaging the O-rings. A very small amount of lubricating grease was applied prior to assembly and was carefully wiped off to leave only a minute amount of grease. This procedure is, however, not very accurate and may explain the relatively wide scatter of the results. An attempt was made to use a split ring for the mass in order to avoid the above mentioned difficulties. However, the O-rings were pinched at the split and therefore the idea was not further pursued.

Concluding Remarks

A test procedure is described which provides results for the stiffness and damping coefficients of elastomer O-rings subjected to small amplitude reciprocating motion. A wide range of the important parameters affecting the dynamic properties of O-rings can be tested, using this procedure, and

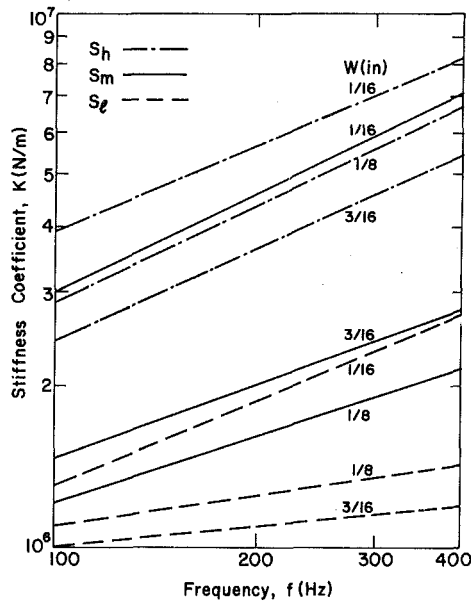


Fig. 4(a) Effect of squeeze, S , on the stiffness coefficient, K , of Viton-75 O-rings, $P = 0.0$

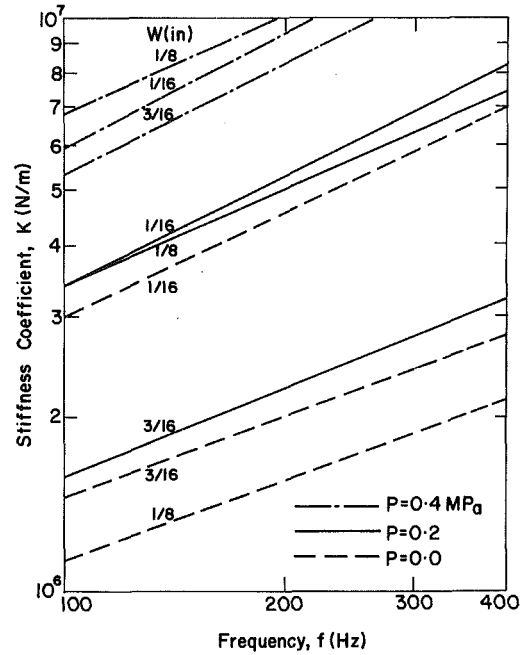


Fig. 5(a) Effect of pressure, P , on the stiffness coefficient, K , of Viton-75 O-rings, $S = S_m$

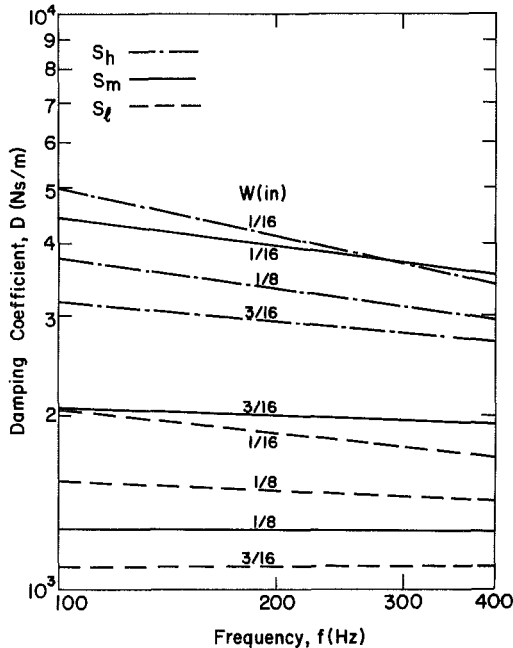


Fig. 4(b) Effect of squeeze, S , on the damping coefficient, D , of Viton-75 O-rings, $P = 0.0$

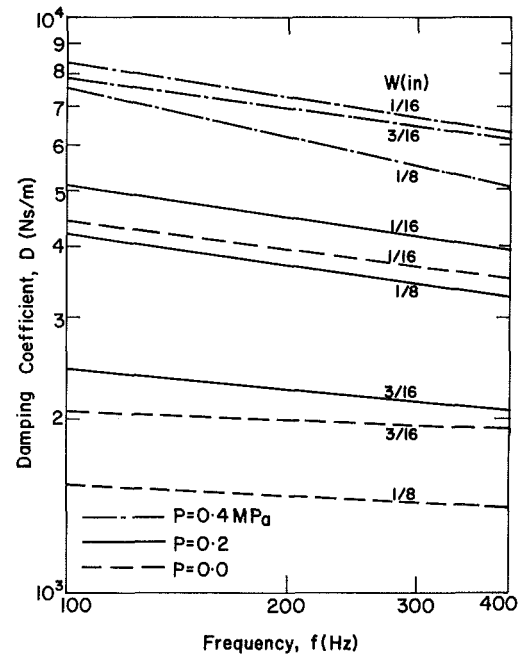


Fig. 5(b) Effect of pressure, P , on the damping coefficient, D , of Viton-75 O-rings, $S = S_m$

analyzed in a relatively short time. A particular test is described aimed at studying the effect of squeeze and pressure on the stiffness and damping coefficients. It is found that increasing the squeeze level or the system pressure increases both the stiffness and the damping coefficients. However, a change in squeeze or pressure level has a little effect on the exponents B , and b used in the empirical expressions of equations (5) and (6). It also seems that the size of the O-ring cross section diameter has little effect on the stiffness and damping coefficients, but because of the irregular behavior of the smallest cross section size O-rings this point has to be further investigated. It will be advantageous in future work to eliminate the uncertainty introduced by sliding the mass over the O-rings for assembly. A more sophisticated design of a splitting ring that does not harm the O-rings may be very helpful.

With the present system having a mass of about 2kg only (because of shaker limitation) the transmissibility α , became

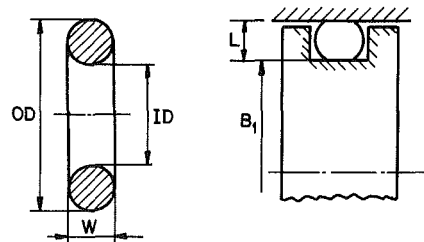


Fig. 6 O-ring and groove dimensions

too small to measure as the stiffness of the O-rings increased. This limited the test to pressures of up to 0.4 MPa only. In order to develop useful data above this pressure range a more powerful shaker and a larger mass are required.

Acknowledgment

The work reported here was supported by RAFAEL-Armament Development Authority under contract No. 3812440.

References

- 1 Darlow, M., and Zorzi, E., "Mechanical Design Handbook of Elastomers," NASA CR 3423, June 1981.
- 2 Smally, A. J., Darlow, M. S., and Mehta, R. K., "The Dynamic Characteristics of O-rings," *ASME Journal of Mechanical Design*, Vol. 100, No. 1, Jan. 1978, pp. 132-138.
- 3 Kazimiersky, Z., and Jarzecki, K., "Stability Threshold of Flexibly Supported Hybrid Gas Journal Bearings," *ASME JOURNAL OF LUBRICATION TECHNOLOGY*, Vol. 101, No. 4, Oct. 1979, pp. 451-457.
- 4 Kittmer, C. A., and Metcalfe, R., "An Inside View of Rotary Seal Dynamics," *Proc. of the 5th Symp. on Engrg. Applications of Mechanics*, Univ. of Ottawa, June 1980.
- 5 Wensel, R. G., et al., "Friction and Axial Force/Displacement Characteristics of Elastomer Seals in Water," ASLE Paper No. 84-LC-6A-1, Oct. 1984.
- 6 Green, I., and Etsion, I., "Stiffness and Damping Characteristics of Elastomer O-rings Secondary Seals Subjected to Reciprocating Twist," *Proc. 10th Int. Conf. on Fluid Sealing*, BHRA, Apr. 1984, pp. 221-229.
- 7 O-ring Handbook, Parker Hannifin Corp. O-ring Division.
- 8 Bendat, S. J., and Piersol, G. A., *Random Data: Analysis and Measurement Procedures*, Wiley, New York, 1971.

APPENDIX A

Effective Squeeze

Consider the O-ring shown in Fig. 6, the nominal squeeze is defined as

$$S = \frac{W-L}{W}$$

where W is the free cross section diameter. The stretch is defined as

$$S_t = \frac{B_1 - ID}{ID}$$

where B_1 is the groove diameter over which the O-ring is stretched and ID is the free O-ring inner diameter. Stretching the O-ring reduces its cross section diameter from W to d according to

$$\frac{W-d}{W} = \nu \frac{l_e - l}{l}$$

where l_e , the O-ring length after stretching, and l , its free length are approximated by $l_e = \pi B_1$ and $l = \pi ID$, respectively. Hence, for an incompressible material with a Poisson ratio $\nu = 0.5$ we have

$$\frac{d}{W} = 1 - 0.5S_t$$

The effective squeeze presented in Table 1 which accounts for the reduction in the cross section diameter is

$$S = \frac{d-L}{d} = 1 - \frac{L}{d}$$

or

$$S = 1 - \frac{L}{W(1 - 0.5S_t)}$$

APPENDIX B

Spectral Analysis

The background for the spectral analysis used in the present work can be found in Chapters 1, 3, 5, and 9 of reference [8].

The Fourier transform of a signal $x = x(t)$ sampled in the time interval $0 < t < T$ is

$$X = (f, T) = \int_0^T x(t) e^{-i2\pi ft} dt$$

For a specific discrete set of N frequencies

$$f_k = \frac{k}{Nh}, \quad k=0,1,2,\dots,N-1$$

(h being the fixed time interval between successive samplings) the discrete Fourier transform becomes

$$X_k = \sum_{n=0}^{N-1} x_n \exp\left(-i \frac{2\pi kn}{N}\right) \quad (7)$$

where x_n is the discrete value of $x(t)$ at $t = nh$. Selecting the number N of time intervals, h , between successive samplings in the form

$$N = 2^P$$

where P is an integer, enables the evaluation of (7) by Fast Fourier Transform (FFT) which is a very efficient numerical algorithm.

The Power Spectral Density Function of $x(t)$ is given by

$$p_x(f_k) = \frac{2h}{N} |X_k|^2$$

Similarly for a signal $y = y(t)$ we have

$$p_y(f_k) = \frac{2h}{N} |Y_k|^2$$

where Y_k is calculated according to (7) by replacing X and x by Y and y , respectively.

The Cross Spectral Density Function is given by

$$p_{yx}(f_k) = \frac{2h}{N} Y_k^* X_k$$

where Y_k^* is the conjugate of Y_k . p_{yx} can also be represented in the complex form

$$p_{yx}(f_k) = C_{yx}(f_k) - iQ_{yx}(f_k)$$

If the signals $y(t)$ and $x(t)$ represent the base motion and the mass response, respectively, then the transmissibility $\alpha = x_0/y_0$ is given by

$$\alpha(f_k) = \frac{|p_{yx}(f_k)|}{p_y(f_k)}$$

and the phase shift is given by

$$\phi(f_k) = \tan^{-1} \left[\frac{Q_{yx}(f_k)}{C_{yx}(f_k)} \right]$$

The Coherence Function is given by

$$\gamma_{yx}^2(f_k) = \frac{|p_{yx}(f_k)|^2}{p_x(f_k)p_y(f_k)} \leq 1$$

and is a criterion for the correlation between $x(t)$ and $y(t)$ at the frequency f_k . If $\gamma^2 = 0$ at a certain frequency than $x(t)$ and $y(t)$ are uncorrelated at that frequency. On the other hand if $\gamma^2 = 1$ at a certain frequency than $x(t)$ and $y(t)$ are fully correlated at that frequency and the response $x(t)$ is a definite outcome of the forcing function $y(t)$. Hence, a coherence function value γ^2 close to unity can serve as an indication for the reliability of the results. It can also be shown [8] that for a linear system represented by constant in time stiffness and damping coefficients the coherence function always gives $\gamma^2 = 1$. Hence, γ^2 close to unity justifies the assumption of a Kelvin-Voigt model with constant in time dynamic coefficients for the O-rings.